Electromagnetic And Thermal (Lumped Circuit) Analysis Of Internal Permanent Magnet Synchronous Machine

Monika Verma[1], Arun Kumar G[2], Ganesh Nagarajan[3]

[1]M Tech, Power Electronics & Drives SELECT, VIT University, Vellore, Tamil Nadu, India
[2]Asst. Professor (Sr.), SELECT, VIT University, Vellore,Tamil Nadu, India
[3]Deputy Manager, CAE-Electric Machines Powertrain Engineering-CAE & TESTING, RNTBCI Pvt Ltd, India

Abstract: *The unique merits of internal permanent magnet synchronous machine (IPMSM) make it a good candidate for automotive industrial applications. This paper presents the design of an internal permanent magnet synchronous machine having fractional slot configuration with single layer concentrated winding arrangement. The electromagnetic analysis has been performed using finite element analysis via ANSYS Maxwell v.2014. Thereafter a lumped parameter thermal network model has been developed for thermal analysis of designed model. The validation of the IPMSM model has been carried out through a few case studies by comparing the respective results.*
Keywords: *IPMSM, finite element analysis, ANSYS Maxwell, lumped circuit thermal network.*

I. Introduction

There are different electrical machines that have been used in automotive application so far, like induction machines, DC machines, permanent magnet machines and switched reluctance machines. Among these, DC machines have been ruled out because of the high maintenance problems associated with its operation. The operation of switched reluctance machines are difficult to control due to which not taken under consideration for such applications. The induction machines are the most interesting machines for automobile applications up to now. However, the PMSMs are the most capable competitor with induction machines for automotive applications due to their many advantages including high efficiency, compactness, high power density, fast dynamics and high torque to inertia ratio. The Internal PMSM having additional features of mechanical robustness, flux weakening capability and high speed operation are particularly suitable for automotive applications.

Different topologies of permanent magnet machines are available e.g. radial flux and axial flux PMSMs. Radial flux PMSMs are the most common due to its simplicity and its similarity with the synchronous AC motors. In this configuration, Internal PMSM exhibit better performance by providing high air gap flux density and also the PMs are protected against demagnetization and mechanical stress.

Proper performance of IPMSMs depends on their optimal design and control. In this paper, an optimized design of internal permanent magnet synchronous machine has been proposed. For this, the design parameters are computed analytically and then optimized on the basis of finite element analysis using ANSYS Maxwell results. After this, thermal nodal network is obtained for thermal analysis. Finally, the model configuration is validated through a few case studies.

II. Machine Model Design

The internal permanent magnet synchronous machines are available in various configurations; among them the one with tangential magnet poles having single barrier structure enjoys many features including structural simplicity, mechanical robustness, good flux weakening capability and high speed range. For winding layout design, the single layer concentrated winding arrangement has been used due to following advantages:

- Electrical separation among the phases (which implies separate source for each phase)
- Physical separation among the phases (which implies a single layer winding with non-overlapped coils)
- Magnetic separation among the phases (which implies a null mutual inductance)

A. Dimensions of rotor, stator, PM, flux barriers

The desired rating parameters of the machine to be designed in this work are:

- Output power, P = 4 kW
- Base speed, ω_b = 3000 rpm

Therefore, the nominal torque to be achieved should be:

$$T = \frac{P}{\omega_b} = 12.73\ Nm$$

The IPMSM model is designed using basic machine sizing equations of the electrical machine [2]. For electrical machines in general, the shear stress [kPa], which expresses the force applied on the conductors, is defined by

$$\sigma = BA$$

Where, B is the magnetic loading (or flux density) and A is the electrical loading (or linear current density). For a radial flux machine, the shear stress is related to the torque by following equation:

$$T = 2V_r\sigma \tag{1}$$

$$V_r = \left(\frac{\pi}{4}\right)D^2L \tag{2}$$

Where, V_r is the volume of rotor, D the rotor diameter and L the rotor stack length. The typical values of σ are shown in table [1].

Table[1]: Typical shear stress values for electrical machines

Application	Shear Stress[kPa]
Industrial motors < 1 kW	0.7 to 2
Industrial motors > 1 kW	4 to 15
High performance industrial servos	10 to 20
Aerospace machines	20 to 35
Very large liquid cooled machines	70 to 100

For the motor design, following values have been considered as the starting parameters:

- Shear Stress, σ = 10 kPa
- Rotor dimensions ratio, D/L = 0.8
- Air gap length, δ = 0.5 mm
- Air gap flux density, B = 0.8 T
- Maximum stator yoke flux density, B_y = 1.4 T

From equations (1) and (2), rotor dimensions are calculated as:

$$D = 86.549 \text{ mm}$$
$$L = 108.187 \text{ mm}$$

With reference to [2], the torque optimum is reached when the ratio of the stator slot inside to outside diameter is 0.7. Hence, the stator slot outside diameter and slot height are calculated as:

$$D_{sl} = \frac{D + \delta}{0.7} = 124.355 \text{ mm}$$

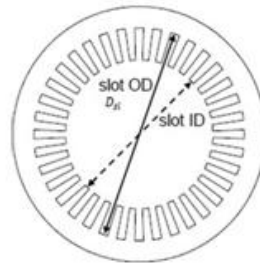$$h_{sl} = \frac{D_{sl} - (D + \delta)}{2} = 18.653 \text{ mm}$$

Fig. 1.   Stator slot outside diameter D_{sl}

The stator yoke thickness is calculated as:

$$t_{sy} = \frac{B}{B_y}\frac{\pi}{4}\frac{D}{\left(\frac{P}{2}\right)} = 7.768 \text{ mm}$$

The outer stator diameter is calculated as:

$$D_{out} = D + 2(\delta + h_{sl} + t_{ys}) = 140.391 \text{ mm}$$

For the initial design of the stator frame, the sides of the stator slots are considered to be parallel. The slot structure will be one of the object for optimization later on.

B. PM and flux barrier dimensions

The purpose of permanent magnet is to provide magnet torque in the total torque contribution by the motor. The Internal PMSM configuration chosen for this work has a structure with NdFe35 permanent magnets

with single flux barrier rotor structure. The initial dimensions of PM as well as of the flux barriers are given below:

* PM dimensions, $l_m \times w_m = 6mm \times 12mm$
* Flux barrier dimensions,
  $h_1 = 10.29mm, h_2 = 4.29mm, d = 3.10mm, t =$
* $1.72mm, \alpha = 117.75^0$
  Positioning of PM, $\gamma = 34mm$

These parameters will be utilized for optimization purpose with the clear aim of obtaining best performance out of the initially designed model. The fig. 2 mainly details the rotor configuration and dimensions as the stator configurations are already discussed in the previous section.
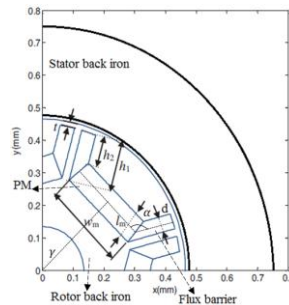
Fig. 2.   Rotor configuration of the interior PMSM

C. Winding arrangement

The design of a single layer concentrated winding and a pole/slot combination of 10/12 (i.e., 10 poles and 12 slots) is proposed in this paper. This combination has been widely tested and presents the following features:

* High fundamental winding factor (k_{wf}=0.933)
* High $LCM\ (Q, P) = 60$ (Least Common Multiple)
* Unbalanced magnetic pull is not present, $GCD\ (Q, P) = 2$ (Great Common Divisor)
  This winding is characterized by slots per pole per phase given by:

$q = \dfrac{Q}{mP} = 2/5$

Where, Q represents the number of stator slots, m the number of phases and P the number of poles. The periodicity of the machine is

$t = GCD\left(Q, \dfrac{P}{2}\right) = 1$

i.e., the machine is odd periodic. The winding design is hereafter obtained by the 'Star of Slots' method. The necessary feasibility check gives a positive result since

$\dfrac{Q}{mGCD\left(Q, \frac{P}{2}\right)} = 4$

is an integer value. For the double layer concentrated winding, the star of slots is composed of $Q/t = 12$ spokes. The angle between the phasors of two adjacent slots is

$\alpha_s = \dfrac{\pi P}{Q} = 150°$

The angle between spokes is

$\alpha_{ph} = \left(\dfrac{\alpha_s}{P/2}\right) t = 30°$

Since the periodicity of the machine is odd, in the transformation from double layer to single layer concentrated winding, the spokes of the star of slots are removed alternately, and the resulting star of slots shows a halved number of spokes, i.e., $Q/2t = 6$. Fig. 3 depicts the transformation and resulting star of slots. The single layer concentrated winding layout is as shown in fig. 4.
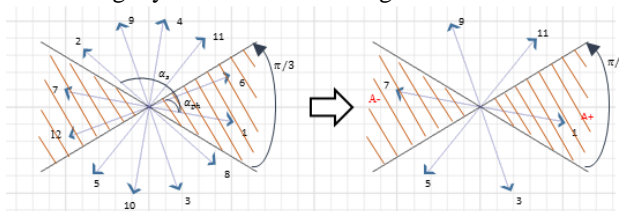

Fig. 3.   Transformation of star of slots of double layer concentrated winding to single layer concentrated winding

Fig. 4.   Winding layout for single layer concentrated winding for Q = 12 and P = 10

This winding arrangement will be validated via simulation of the initial motor design.

III.   Electromagnetic Analysis Results

D. Initial model simulation

Considering all the parameters, the initial motor design PMSM-1 is shown in fig. 5. This model design has been simulated by the means of FEA at its nominal working point to verify the validation of winding arrangement layout discussed earlier. The excitation angle is taken as 10° and the number of stator winding turns per slot is considered to be 55 for PMSM-1 model simulation.
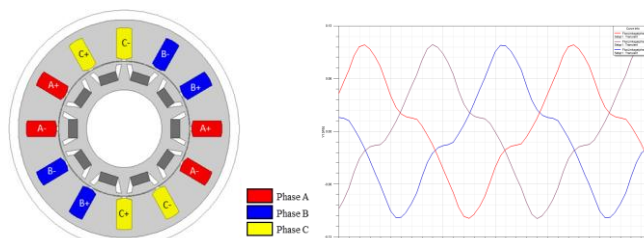
Fig. 5.   PMSM-1 model and flux linkage response

From the simulation results of flux linkages in the windings (fig. 5), it is clear that the flux linkage is sinusoidal with 120° phase shift among the phases. Hence, the model PMSM-1 is validated with the designed winding arrangement. The negative torque value of 5.25 Nm is obtained with the initial model. From now onwards, the parameters of this designed model will be optimized one by one and the model will be refined in order to obtain the desired torque value.

E. Optimization and refinement

The optimization and refinement of the designed model is done based on the number of turns in the stator winding, angle of excitation, slot structure, stack length, positioning & dimensioning of permanent magnet and flux barrier structures in the motor using Finite Element Analysis.

Fig. 6 shows the variation of the torque with excitation angles and the corresponding Torque-Voltage (TV plot) curve for the model.
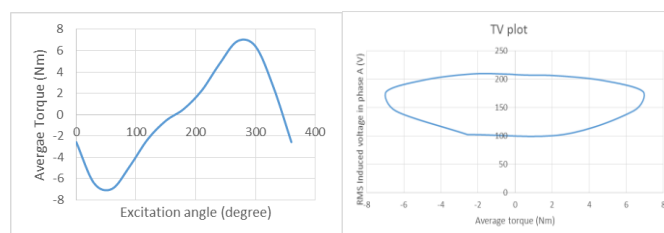
Fig. 6.   Torque variation with excitation angle and TV plot

The maximum torque is obtained at the excitation angle of 270°. However, the torque value recorded (8.32Nm) is far away from the target value. Hence, further modifications are done in the designed model with respect to the other parameters in order to get the desired performance of the machine. An optimization process is performed in order to find the best combination among the following parameters:

- The stator winding number of turns per slot, (50)
- PM dimensions, (8mm×19mm)
- Flux barrier dimensions,
  $h_1 = 8.23mm, h_2 = 0.5mm, d = 1.55mm, t = 1.74mm, \alpha = 99.89^0$
- Positioning of PM, $(\gamma = 37mm)$

The refined model PMSM-2 and the corresponding torque simulation result is shown in the fig. 7. Here, the average value of torque is recorded as 16.42 Nm.
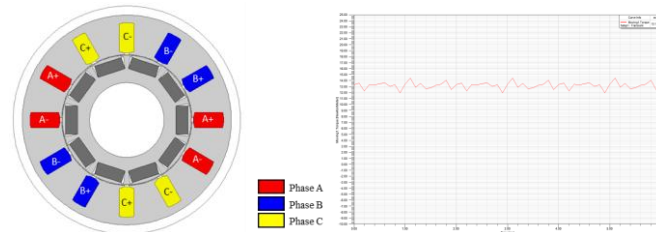
Fig. 7.   PMSM-2 model and torque simulation result

This optimization process led to the decreased number of winding turns and increased value of reluctance as well as magnetic torque capability of the machine with decreased amount of the copper usage.

The simulations are now carried out with decreased length of the machine (100mm). The lesser the stack length, lesser are the stranded losses in the machine. Holes are added in the rotor structure geometry to increase the saliency. The new model is named as PMSM-3. In PMSM-3, the sides of the teeth are taken parallel (earlier slot sides were parallel). This way more of the stator core material is exploited. The more refined and optimized model is shown in the fig. 8.
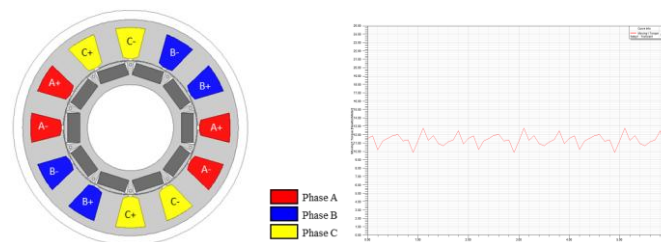
Fig. 8.   PMSM-3 model and torque simulation result

In PMSM-3, the shaft diameter is changed to 56 mm so that the q-axis insulation ratio has now become $k_{wq} = 0.96$ [6]. This refinement further reduces core material. Next, the torque-voltage curves for different current values with fixed number of turns and stack length are compared (fig. 9). Here, the parametric analysis is carried out with three distinct values of currents; i.e. $11.66\,A, 12.83\,A$ and $14\,A$. By varying the excitation angle from 210^0 to 360^0, the corresponding TV curves are plotted as shown in the fig. 9:
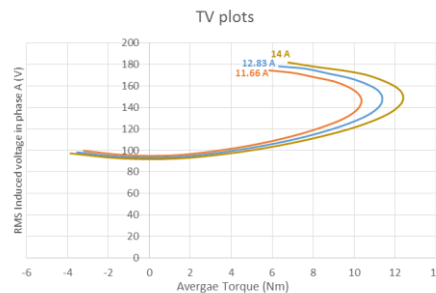
Fig. 9.   TV plots for PMSM-3 for three different currents

It can be seen that the TV circular plots are expanding with the increase in current value.

From now onwards, the TV plots are studied with different electrical loadings and hence, the refinement of the model PMSM-3 will be done on the basis of the observations from the plots. In the parametric analysis of PMSM-3, the stator winding number of turns per slot is varied from 38 to 46 with the step value of 2 and the stack length is varied from 90 mm to 110 mm with the step of 10 mm and TV curves are plotted for three values of currents; i.e. $11.66\,A, 12.83\,A$ and $14\,A$. The TV plots can be seen in the following figures.
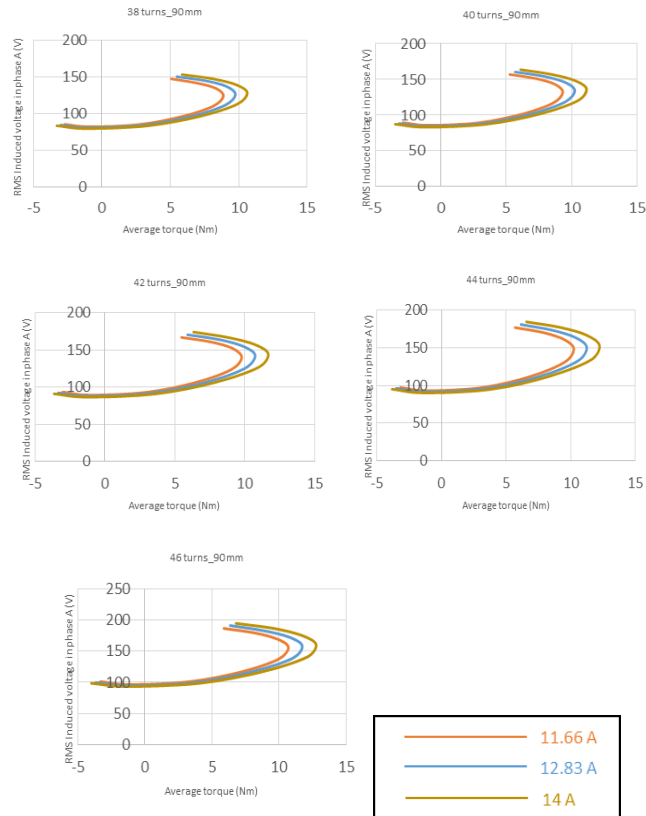
Fig. 10. TV plots for different turns with 90 mm stack length
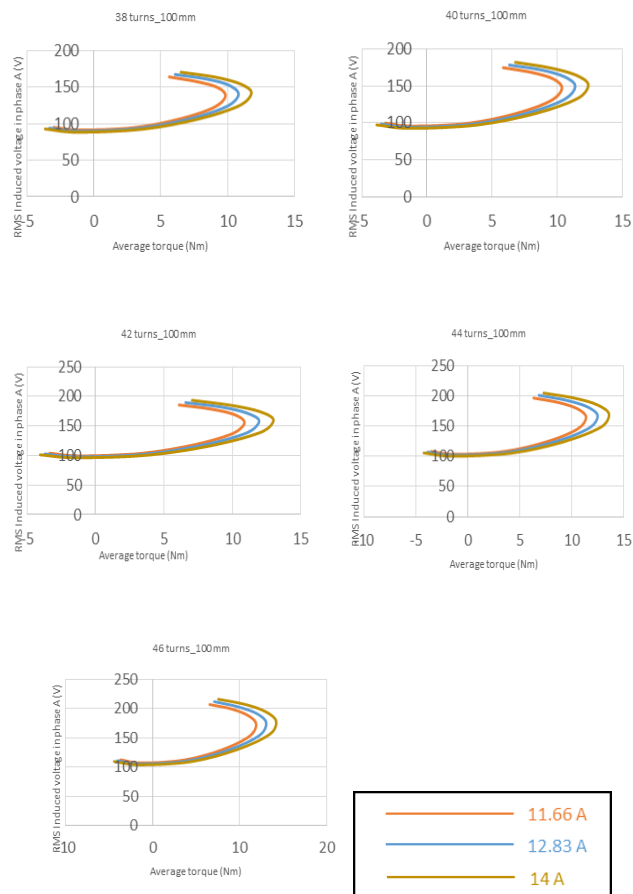

Fig. 11. TV plots for different turns with 100 mm stack length
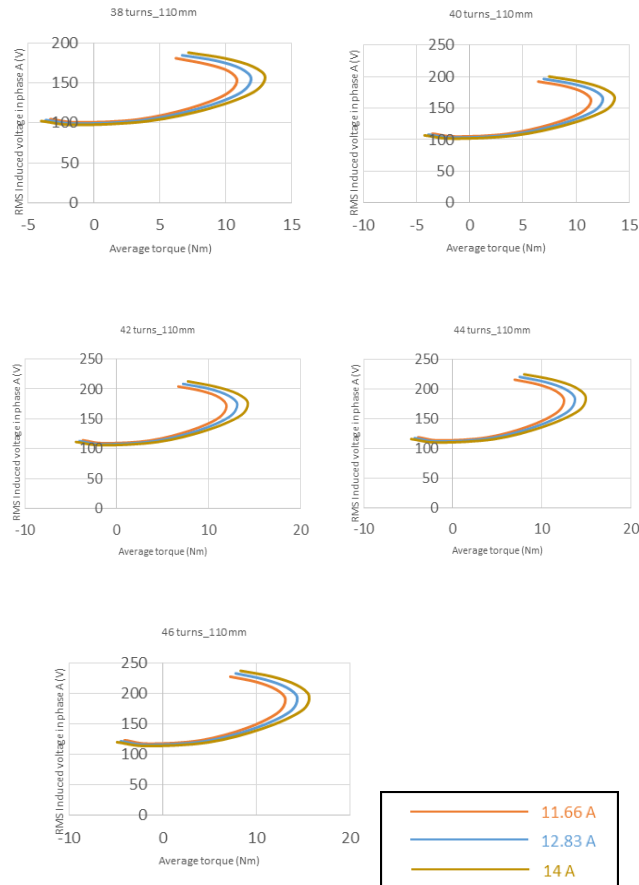
Fig. 12. TV plots for different turns with 110 mm stack length

Hence, the initially designed model has been optimized to obtain the required nominal torque (≈13Nm). In the whole process, the negative torque of 5.25 Nm has been improved to reach the target value of 12.94 Nm. The torque response and rms induced voltage for the model are shown in fig. 13. The flux linkage and induced currents are also shown in the fig. 14.
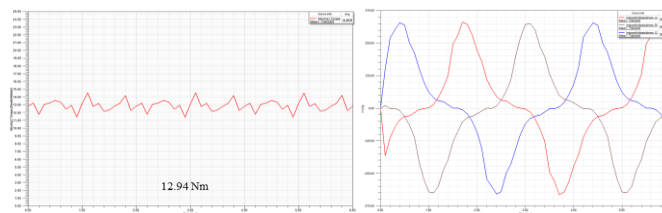
Fig. 13. Torque and induced voltage for IPMSM model
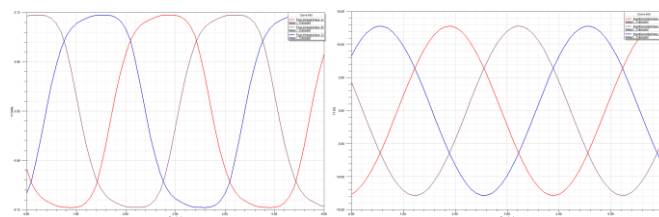
Fig. 14. Flux linkage and induced current for IPMSM model

The magnetic flux density and the flux lines distribution for the model IPMSM are represented in the fig 15.
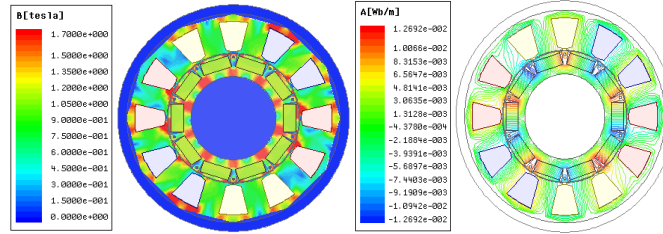
Fig. 15. Magnetic flux density and Flux lines distribution for IPMSM model

IV.   Lumped Parameter Thermal Nodal Network

The principle of lumped circuit thermal analysis is to develop an electrical equivalent circuit for thermal analysis. Each node of the circuit represents a part of the machine. Each node is connected to other nodes via thermal resistances through which heat can flow.

The conductance matrix, G of a system consisting of n+1 nodes is represented as:

$$G = \begin{bmatrix} \sum_{i=1}^{n} \frac{1}{R_{1,i}} & \frac{-1}{R_{1,2}} & \cdots & \frac{-1}{R_{1,n}} \\ \frac{-1}{R_{2,1}} & \sum_{i=1}^{n} \frac{1}{R_{2,i}} & \cdots & \frac{-1}{R_{2,n}} \\ \cdots & & \cdots & \cdots \\ \frac{-1}{R_{n,1}} & \frac{-1}{R_{n,2}} & \cdots & \sum_{i=1}^{n} \frac{1}{R_{n,n}} \end{bmatrix}$$

The loss vector, P be defined to represent the power loss injected in each node,

$$P = \begin{bmatrix} P_1 \\ P_2 \\ \cdots \\ P_n \end{bmatrix}$$

And corresponding temperature vector, θ representing the increase in temperature compared to the ambient temperature.

$$\theta = \begin{bmatrix} \theta_1 \\ \theta_2 \\ \cdots \\ \theta_n \end{bmatrix}$$

The temperature θ can be calculated by inverting the conductance matrix and multiplying it with the power loss vector,

$$\theta = G^{-1} P$$

A simple thermal network model is proposed. The idea is to model the different heat flow paths in the motor and the associated resistances. The node placement excludes the non-radial phenomena. Fig. 16 shows how the nodes have been placed in the model geometry and hence the lumped parameter equivalent thermal model is shown. The corresponding thermal resistances are tabulated in the table [2].

Loss simulation results

By Loss analysis using ANSYS Maxwell v.2014, the simulation results are shown in fig. 17.
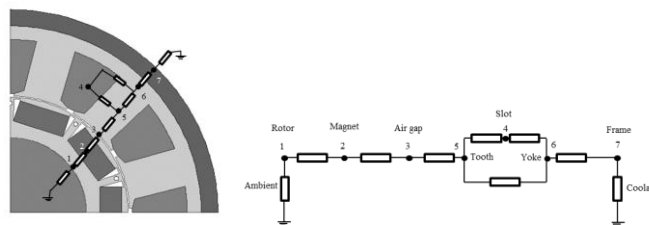
Fig. 16. Node location in geometry of model & lumped parameter thermal nodal network.

Table [2]: Thermal resistances connecting the nodes

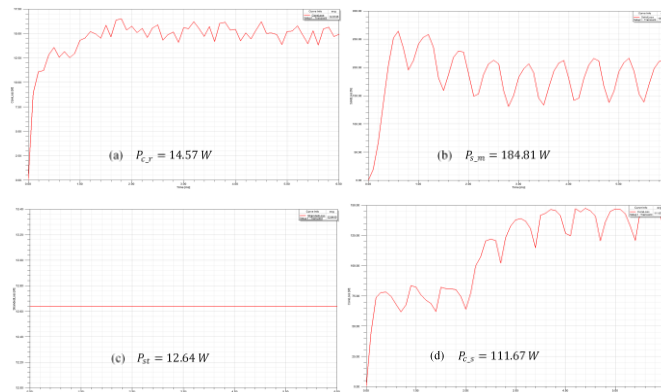| node 1	node 2	Thermal resistance values (K/W)
Rotor	Magnets	0.250222109
Magnets	Air gap	0.640277373
Air gap	Tooth	0.275061
Slot	Tooth	0.003937138
Slot	Yoke	0.0560443
Tooth	Yoke	0.298007
Yoke	Frame	0.00246402
Frame	Coolant	0.00032502

Fig. 17. Loss simulation results in (a) rotor (b) magnets (c) slots and (d) stator

Loss input

The power loss vector (in watts) corresponding to each node is given below:

$$P = \begin{bmatrix} P_1 \\ P_2 \\ P_3 \\ P_4 \\ P_5 \\ P_6 \\ P_7 \end{bmatrix} = \begin{bmatrix} 14.57 \\ 184.81 \\ 3.23 \\ 12.64 \\ 70.53 \\ 41.13 \\ 0 \end{bmatrix}$$

The temperature vector θ in °C, representing the increase in temperature compared to the ambient temperature.

$$\theta = G^{-1}P = \begin{bmatrix} \theta_1 \\ \theta_2 \\ \theta_3 \\ \theta_4 \\ \theta_5 \\ \theta_6 \\ \theta_7 \end{bmatrix} = \begin{bmatrix} 102.07 \\ 123.75 \\ 53.12 \\ 89.84 \\ 119.86 \\ 104.93 \\ 6.38 \end{bmatrix}$$

Hence, the lumped parameter model with each node temperature is as shown in the fig. 18:
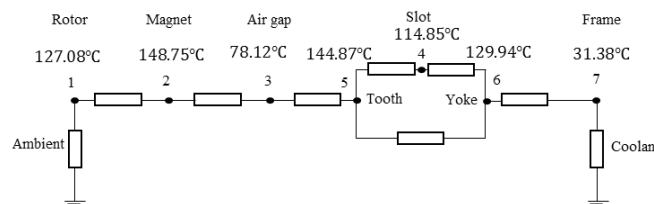
Fig. 18. Lumped parameter thermal network with temperature distribution

Table [3] shows the output of nodal temperature distribution with the corresponding permissible limits.

Table [3] Thermal analysis results comparison

Node no	Node component	Component material	Temperature obtained (°C)	Permissible temperature (°C)
1	Rotor	M400-50A1	127.08	162
2	Magnet	NdFe35	148.75	150
3	Airgap	Air	78.12	-
4	Slot	Copper	114.85	165
5	Tooth	M400-50A1	144.87	162
6	Yoke	M400-50A1	129.94	162
7	Frame	Aluminum	31.38	100

It can be seen that the temperatures of the different parts of the machine are under safe thermal limits.

V. Case Studies For Validation Of Model Configuration
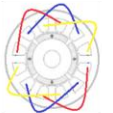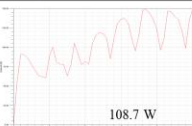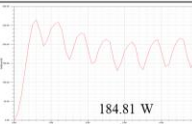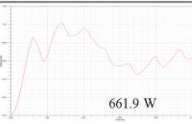
Here, the feasibility of proposed topology for IPMSM is discussed and different case studies are carried out to check the performance of the machine with the selected configuration. Thus the designed machine model is validated with the help of the respective results.

F. Case study (I): Efficiency test

In order to check efficiency, the stator configuration of IPMSM is examined. Here, testing of the designed model is done with both types of concentrated and distributed winding configuration. The losses and efficiencies in both models are compared. Table [4] gives the comparison of the results for the designed model and the test model. It is to be noted that the test model is having same optimized dimensions of that of the designed model except the winding arrangement, which is distributed in this case.

Hence it is proved using this test that using concentrated winding increases the efficiency in low speed region, where copper loss is more prominent than core loss.
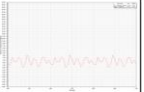
Table [4] Test results for comparison of losses and efficiency

Parameters	Concentrated winding configuration	Distributed winding configuration
Models		
Core loss simulation result	126.24 W	108.7 W
Solid loss simulation result	184.81 W	661.9 W
Total loss	311.05 W	770.6 W
Efficiency	92 %	80.4 %

G. Case study (II): Test for noise and vibration

The problems of vibration and noise production in the machine mainly arise due to the torque ripple and cogging torque. Fractional pitch winding configuration is recommended so as to obtain minimum cogging torque. With this, the torque ripples are also reduced, thereby decreasing the problems of vibrations in the machine. So, for proving this fact the test model is designed with full pitch winding configuration with 24 slots, 8 pole combination. The simulations are done to compare the results of torque ripple and cogging torque value of both the models.

Table [5] Vibration and noise reduction test results

Parameters	Fractional pitch winding	Full pitch winding
SPP (Slots per Pole per Phase)	2/5	1
Models	Slots=12 Poles=10	Slots = 24 Poles = 8
Torque ripple simulation result		
Cogging torque simulation result		
Torque ripple	0.24 p.u.	9.61 p.u.
Cogging torque (mNm)	5.9	42

From the table [5], it can be seen torque ripple and cogging torque in the model with fractional pitch winding is much lesser than that obtained from the model with full pitch winding. Fractional slot winding configuration not only reduces noise in the machine but it also helps the machine to become more fault tolerant. This property is discussed in the upcoming section with the help of a separate test.

H. Case study (III): Fault tolerance testing

The given test is carried out to compare the mutual inductances among the phases in both types of the machine; one with fractional pitch winding and another with full pitch winding configuration. The simulations are done using Magnetostatic solver in Maxwell to compute the post processed inductance matrix for three phase windings. Table [6] shows the inductance matrix for both the models.
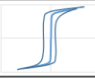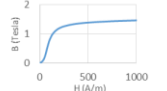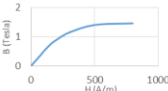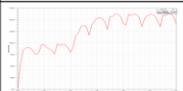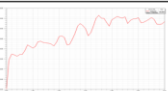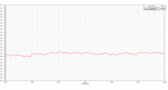
Table [6] Fault tolerance test results

Parameters	Fractional pitch winding	Full pitch winding
SPP (Slots per Pole per Phase)	2/5	1
Inductance matrix simulation result (mH)	A B C A 543.57 -251.59 -185.46 B -251.59 368.2 151.8 C -185.46 151.8 224.15	A B C A 498.18 -307.13 -306.16 B -307.13 716.75 408.31 C -306.16 408.31 462.48
Mutual inductance	Lesser	More

It can be seen from table [6], the machine designed in this project with fractional slot configuration is having almost half mutual inductance values as compared to the test machine model having full pitch winding configuration. Hence, the effects of the faulty conditions in one phase will be lesser on neighboring phases. In simpler words, the machine with fractional slot configuration is more fault tolerant.

I. Case study (IV): Core loss reduction test

Table [7] Core material test results

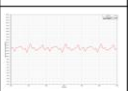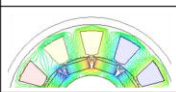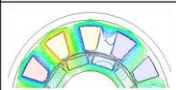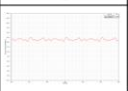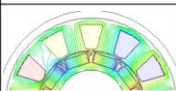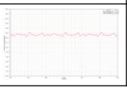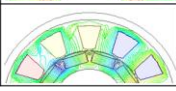| Parameters	Core material with narrow hysteresis loop	Core material with wide hysteresis loop
Hysteresis loop	Narrow	Wide
BH curve		
Core loss simulation result		
Torque simulation result		
Core loss value	126.24 W	139.95 W
Torque value	12.82 Nm	8.85 Nm
Conclusion	Lesser loss, more torque	More loss, lesser torque

The core losses occur in the machine mainly due to the improper selection of the core material. Therefore, an appropriate choice of material which has a narrower hysteresis loop and the ability to be made into very thin laminations is desired. Non-oriented (N.O.) silicon sheet steel is the most common choice which is made for the machine model used in this work. A simple test is carried out by taking a test core material which exhibit wider hysteresis loop. Thus, the core losses are compared for two models to check the performance of the machine with two different materials.

The machine using core material with narrower hysteresis loop possess lesser core loss and more torque output whereas the performance with wider hysteresis core material lesser torque is obtained with more losses in the core. Therefore, this test gives favorable results for the machine performance.

J. Case study (V): Performance of motor with different permanent magnets

The purpose of permanent magnets in the IPMSM machines is to provide the necessary rotor flux which has to be stationary with respect to stator mmf to produce the steady state torque. As the necessary torque produced by the motor has been the main designing criteria in this work, hence the torque produced by the machine with different permanent magnets are compared by this test. Also the flux linkages are compared with different magnets. Table [8] shows the flux lines plots and torque simulation results produced by the model with different magnets in the rotor.

Table [8] Test results for the model with different magnets

Permanent Magnet Type	Torque value	Flux linkage value	Torque simulation results	Flux linkage simulation results
NdFeB	12.94 Nm	0.0126 Wb/m		
Ferrite	0.0177 Nm	0.0065 Wb/m		
SmCo	11.3 Nm	0.0115 Wb/m		
Alnico	11.6 Nm	0.0117 Wb/m		

As can be observed from the test results, the best performance is given by the NdFeB magnets which is used in this thesis work. The worst performance is given by the ferrite magnets if would have been used in the designed model. However, SmCo and Alnico magnets are producing almost the same torque and flux linkages. The Samarium Cobalt magnets are costlier than NdFeB magnets. And Alnico magnets despite being oldest commercially available magnets have relatively low magnetic values because their ease of demagnetization. Hence, NdFeB magnets are the recommended magnets for the proposed topology of the IPMSM model.

VI.   Conclusion

IPM technology is taking several industries by storm. It is compact, light, efficient, reliable and can be used in divert craft system. In this paper, an optimal and accurate design of internal permanent magnet synchronous machine with single layer, fractional slot concentrated winding and single flux barrier rotor structure has been proposed.

The number of turns in the stator winding, angle of excitation, slot structure, stack length, positioning & dimensioning of permanent magnet and flux barrier structures in the motor using Finite Element Analysis has been chosen as the optimization criteria. For this purpose, the analytical model is designed and hence analyzed to get the best performance out of the optimized design. Thereafter, a lumped parameter thermal nodal network is designed to perform thermal analysis of the model. A few case studies were performed over the machine configuration to check and validate the model configuration. Comparison of results show the validity of analytical design.

References
[1].   "Electric Motor Drive Selection Issues for HEV Propulsion Systems: A Comparative Study" M. Zeraoulia1, Student Member, IEEE, M.E.H. Benbouzid1, Senior Member, IEEE, and D. Diallo2, Member, IEEE 1Laboratoire d'Ingénierie Mécanique et Electrique (LIME), IUT of Brest, University of Western Brittany Rue de Kergoat – BP 93169, 29231 Brest Cedex 3, France
[2].   "Sizing of Electrical Machines", PEBN #9 (26 Sep 2008), W.L. Soong, School of Electrical and Electronic Engineering, University of Adelaide, Australia, soong@ieee.org
[3].   "Use of the star of slots in designing fractional-slot single-layer synchronous motors", N. Bianchi and M. Dai Pr!e
[4].   ANSYS Maxwell 2D Field Simulator v14 User's Guide, ANSYS Maxwell V16 Training Manual.
[5].   "Design of a permanent magnet synchronous machine for the hybrid electric vehicle", World academy of Science, engineering and Technology, Vol: 2, No:9, 2008, Arash Hassanpour Isfahani and Siavash Sadeghi.

[6]. Design and Analysis of a Fractional-Slot Concentrated-Wound PM-Assisted Reluctance Motor, LUIGI MARINO, , KTH royal institute of technology, electrical engineering.
[7]. "Lumped Parameter Thermal Modelling of Electric Machines", Analysis of an Interior Permanent Magnet Synchronous Machine for Vehicle Applications, Bjorn Andersson, division of electric power engineering, Chalmers university of technology, Goteborg, Sweden.
[8]. Thermal Network Modeling Handbook, K&K Associates, Version 97.003, Nation Aeronautics and Space Administration. 1976.
[9]. "Challenges and solutions for IPMSM to be used as a next generation electrical machine", Shah Asifur Rahman, Proceedings of the 2011 international conference on industrial engineering and operations management, kuala lumpur, Malaysia, January 22-24, 2011.
[10]. IPM technology, by Atlas Copco, https://www.youtube.com/watch?v=1bV8W5DZCIQ&spfreload=10
[11]. Ash woods IPM motors, https://www.youtube.com/watch?v=Xsuhk9WVm7Q